ARL-FLIGHT-MECH-R-188

AR-006-149

P-35

DEPARTMENT OF DEFENCE

DEFENCE SCIENCE AND TECHNOLOGY ORGANISATION

AERONAUTICAL RESEARCH LABORATORY

MELBOURNE, VICTORIA

Flight Mechanics Report 188

F/A-18 1/9TH SCALE MODEL TAIL BUFFET MEASUREMENTS

by

C.A. MARTIN, M.K. GLAISTER, L.D. MacLAREN *(ARL)*

L.A. MEYN, J. ROSS *(NASA AMES)*

Approved for public release

JUNE 1991

DEPARTMENT OF DEFENCE
DEFENCE SCIENCE AND TECHNOLOGY ORGANISATION
AERONAUTICAL RESEARCH LABORATORY

Flight Mechanics Report 188

F/A-18 1/9TH SCALE MODEL TAIL BUFFET MEASUREMENTS

by

C. A. Martin, M. K. Glaister, L. D. MacLaren
Aeronautical Research Laboratory

L. A. Meyn, J. Ross
NASA Ames Research Center

SUMMARY

Wind-tunnel tests have been carried out on a 1/9th scale model of the F/A-18 at high angles of attack to investigate the characteristics of tail buffet due to bursting of the wing leading edge extension (LEX) vortices. The tests were carried out at the Aeronautical Research Laboratory low-speed wind-tunnel facility and form part of a collaborative activity with NASA Ames Research Center, organised by The Technical Cooperative Programme (TTCP). Information from the programme will be used in the planning of similar collaborative tests, to be carried out at NASA Ames, on a full-scale aircraft. The programme covered the measurement of unsteady pressures and fin vibration for cases with and without the wing LEX fences, designed by McDonnell Aircraft Company, fitted. Fourier transform methods have been used to analyse the unsteady data, and information on the spatial and temporal content of the vortex burst pressure field has been obtained. Flow visualisation of the vortex behaviour was carried out using smoke and a laser light sheet technique.

POSTAL ADDRESS: Director, Aeronautical Research Laboratory,
506 Lorimer Street, Fishermens Bend, Victoria, 3207, Australia

Contents

List of Figures

1 Introduction

The use of leading edge extensions (LEX's) on the F/A-18 wing to provide vortex lift, coupled with a tail configuration designed to provide directional stability at high angles of attack, provides the aircraft with considerable low-speed, high angle of attack combat capability. An unfortunate consequence of this capability results from the breakdown, or bursting, of the LEX vortices ahead of the tail. Breakdown of the vortex structure produces a high energy, unsteady pressure field which imposes large buffet loads at the tail. In particular, at certain angles of attack, the LEX vortex burst on the F/A-18 produces large vibrations of the fin resulting in heavy fatigue damage and a reduction in structural life. The severity of the F/A-18 fin buffet has been reduced by the installation of a 'fence' designed by McDonnell Aircraft on the upper surface of the LEX which modifies the nature of the vortex breakdown. Although a significant improvement in predicted structural life has been achieved with this modification, more effective solutions are being sought, both for the F/A-18 and for other aircraft designs which rely on vortex lift for high angle of attack capabilities. An important step in this process is the development of a better understanding of the flow behaviour involved in vortex breakdown and of the conditions which lead to tail buffet.

Research into this problem is being carried out in a number of organisations (References [1] and [2]) and active collaborations have been arranged through the TTCP panel HTP-5 on 'manoeuvring aerodynamics'. In support of The Australian Defence Force operations of the F/A-18, and also as part of the TTCP collaboration, a test programme was carried out on a 1/9th scale model of the F/A-18 in the $9' \times 7'$ low-speed wind tunnel at the Aeronautical Research Laboratory (ARL) to measure the flow conditions and fin response due to the vortex burst. The programme was designed to characterise the nature of the vortex burst and associated structural interactions and also to provide background information to support a full-scale wind tunnel test programme to be carried out jointly by NASA and ARL on a F/A-18 in the $80' \times 120'$ wind tunnel at NASA Ames.

Sections 2, 3 and 4 of the report cover the wind tunnel model, the test equipment and the test procedures respectively. Analysis of the unsteady data has been carried out using Fast Fourier Transform (FFT) methods to provide frequency content and correlation information. Details of the analysis and of the presentation of results is covered in Section 5. A discussion of the results, covering six aspects of the tests is presented in Section 6.

2 Wind Tunnel Model Description

A 1/9th scale model of the F/A-18 aircraft was constructed at the Aeronautical Research Laboratory for testing in the Laboratory's low-speed wind tunnel. The model scale was determined by the need to test to an angle of attack of 40° within the physical constraints of the wind tunnel working section. Carbon fibre was used extensively for fabrication of the fuselage and flying surfaces. All flying surfaces were reinforced with high tensile aluminium spars, which also formed the structural sub-frame and load attachment points of the model. Any remaining voids in the flying surfaces were filled with glass fibre mat and casting resin to prevent 'oil-canning' of these relatively planar surfaces. No additional reinforcement was required for the fuselage, the strength and stiffness of the carbon reinforced plastic proving sufficient. This construction method allowed easy access to the inside of the fuselage skin for the placement of pressure taps. With the moulds

constructed, rapid replication and replacement of any part of the model is possible, should the need arise.

For the present investigation, a wing with fixed-leading edge (L.E.) flap deflection of 34° was designed. This L.E. flap angle corresponds to the flap setting for flight at angles of attack greater than 25.6° and Mach numbers less than 0.6. A photograph of the assembled model is shown in Figure 1, while Figure 2 illustrates the various sub-assemblies of the model.

For the purposes of this investigation, the port vertical stabilizer was provided with three pairs of pressure tappings. Each pair consisted of tappings located at the same spanwise and chordwise stations but on opposing sides of the fin. This arrangement allowed for the measurement of differential pressure across the fin. A single pressure tapping was made on the outboard side of the fin which was located alongside a fin tip accelerometer and two surface mounted pressure transducers were positioned on the port wing upper surface just below the position of the vortex burst. The pressure tappings and transducer locations are given in Figure 3. Additional pressure ports were included to match those used on a 16% model tested at NASA Langley.

3 Test Equipment and Accuracy

The model was mounted on a pitch/roll rig via a six component strain gauge balance. No forces or moments were measured during the tests, the strain gauge balance merely providing a convenient means of mounting the model. The unsteady pressures and accelerations were measured using a combination of Entrans and Endevco transducers attached to the fin, wing and fuselage upper surfaces. Those mounted on the wing and fuselage being located immediately below the path of the vortex. All output signals from the transducers were recorded and analysed on a Wavetek 804A Fast Fourier Transform (FFT) Analyser. In addition to the above, a small pressure probe was constructed to obtain measurements of unsteady pressures inside the bursting vortex. This probe contained a Kulite XCS-062-5 differential pressure transducer vented to the local flow via four 0.3 mm holes, five probe diameters aft of the nose. The probe could be adjusted to any position within a spatial 'box' approximately 150 mm in the X direction and 100 mm in the Y and Z directions. The probe assembly and mounting configuration is shown in Figure 4.

Prior to the tests, all transducers were calibrated against a Digiquartz pressure reference of known accuracy and checked for thermal drift. All transducers were found to be within 1% of calibration certificate values. Manufacturers calibration certificate values were used for all data reduction during the test.

4 Test Procedure and Test Conditions

The position of the vortex burst was first defined for a range of angles of attack by the introduction of a smoke filament just below the junction of the forward tip of the Leading Edge Extension (LEX) and the fuselage. The vortex structure forward of the burst was examined at a later stage using a laser beam normal to the vortex path. Results of the flow visualisation studies were recorded on video tape. Pressure and acceleration data could be acquired by the Wavetek 804A analyser from four locations at one time. The data were also recorded in analogue form on magnetic tape. For certain tests, the Wavetek's

signal analysis functions were used, and the output was displayed on the fourth channel.

Tests were conducted in the ARL low speed wind tunnel at velocities of 20 to 60 m/sec, corresponding to a dynamic pressure range of 250 to 2200 Pa and Reynolds numbers from 0.54×10^6 to 1.6×10^6 based on the mean aerodynamic chord of the model.

5 Presentation of Results

The analysis of the unsteady measurements has been carried out primarily with the Wavetek 804A analyser at run time. Some of these results have been re-checked post test from the analogue tape records using a Fortran analysis package described in Reference [3]. Because of the large accumulation of data resulting from this form of analysis, only example plots have been included in this report. Salient features of the analysis such as power spectral density peaks and associated frequencies have been extracted using the analyser cursor.

6 Results and Discussion

6.1 Flow Visualisation

A video camera and still photography were used in conjunction with smoke and both incandescent light and laser light sources to record the location of the vortex burst. Examples of the image of the vortex and vortex burst are shown in Figure 5. The point of the vortex burst is taken as the apex of the conical region. All tests were characterised by low frequency unsteadiness in the vortex longitudinal location. Some evidence exists from other unpublished studies and from water tunnel measurements that this unsteadiness is a characteristic of the vortex burst mechanism. For the present study the longitudinal burst position was taken as the mean of the unsteady variation.

Figure 6 shows the vortex burst location plotted as a percentage of model length for cases with and without the fins removed. With the fins removed the vortex burst location moves aft, for the same angle of attack. The movement is greatest at low angles of attack where the burst is closest to the fin leading edge. The vortex burst point is known to depend on the characteristics of the downstream pressure field and these results provide additional information on this dependency.

All measurements in this programme were carried out with natural airflow through the model engine intake. Evidence from Reference [2] indicates that engine intake velocity can affect LEX vortex development and vortex burst location. The value of the engine intake velocity was not recorded in this programme and so care must be taken when comparing the results with those from other models.

6.2 Frequency Characteristics of the Unsteady Pressure Field in the Vortex Burst

Unsteady pressure measurements from two transducers mounted on the port wing surface, and from a pressure transducer and an accelerometer mounted on the port fin, as shown in Figure 3, were analysed to determine the frequency characteristics of the vortex burst.

Typical Power Spectral Density (PSD) results are presented in Figures 7 to 10 for an angle of attack of 26.5° and for a range of tunnel speeds. The PSD plots are the average

of 30 ensembles. The results show that the pressure field due to the vortex burst contains energy over a moderately narrow frequency band. The band width and centre frequency differ slightly between the wing surface and fin locations. However, the overall frequency content is seen to be a strong function of tunnel speed. The centre of the energy band for the rear surface pressure transducer was located visually using the analyser cursor and the results are presented as a function of tunnel speed for a range of angles of attack in Figure 11. The centre frequency increases linearly with increasing tunnel speed, and the gradient increases with decreasing angle of attack. Data from Reference [1], measured on a 12% scale model indicates that the frequency of the vortex burst energy obeys normal frequency scaling laws.

Flow visualisation tests and unsteady surface pressure measurements were also carried out on the model with the fins removed. For this case, Figure 6 shows that the vortex burst point moves further aft for the same angle of attack, while the frequency analysis shows that the centre frequency of the burst increases, (Figure 12). Although the presence of the fin alters the vortex burst location and modifies the frequency of the pressure field, there is no indication, based on the information recorded, that vibration of the fin modifies the frequency content of the pressure field.

From this data, which covers only a few angles of attack, the vortex burst position and the burst frequency show significant correlation. However, both parameters are functions of angle of attack and the underlying dependencies are not yet understood. Further work is being carried out on simple geometries to provide a better understanding of the relationships between the angle of attack and the burst characteristics, such as burst position and burst frequency.

Time correlation calculations were carried out on the signals from the two wing surface pressure transducers which were located 100 mm apart in a streamwise direction. The correlation was calculated by applying an inverse Fourier transform to the cross power spectrum, which had previously been obtained from averaging Fourier transforms of thirty ensembles. The resulting correlation plot provides an estimate of the dominant frequency in the pressure field and also an estimate of the pressure field convection velocity. The frequency estimates agree closely with those obtained from the power spectrum measurements. The pressure field convection velocity is shown in Figure 13 to be 0.4 times the free stream velocity for the case at 23.5° angle of attack and 0.29 free stream velocity for 28.5° angle of attack.

In summary, analysis of the surface pressure measurements shows that with increasing angle of attack, the vortex burst location moves forward and the burst pressure field frequency and convection velocity decrease. When the fins are removed, the burst location moves aft, for a given angle of attack, and the burst frequency increases.

6.3 Vortex Burst Profile from Pressure Probe Measurements

A special purpose pressure probe was manufactured using, as a sensing element, a high frequency pressure transducer (Figure 4). The probe design is similar to that used for free stream static pressure measurements. The pressure probe was traversed parallel to the normal axis, from a position above transducer A (Fig 3) through the centre of the vortex burst. Flow visualisation was used to locate the centre of the vortex burst for an angle of attack of 26.5°. No change in vortex burst position was detected due to the presence of the probe.

It should be noted that because of the large unsteady flow reversals within the vortex burst region, the pressure sensed by the probe will be the sum of the local static pressure plus dynamic components due to cross flow velocities. Nevertheless, it is expected that the mean pressure and the power spectral density results will provide an indication of the extent and intensity of the fluctuating pressure field due to the vortex burst.

Figure 14 shows the peak values of the power spectral density measurements as probe position is moved from a position directly above the wing's rear surface transducer along a path parallel to the normal axis. The profile increases from the value measured by the surface transducer to a peak at a small distance away from the wing surface, then reduces to a minimum value at the position, identified by flow visualisation, as the centre of the burst, and then increases again to a value similar to that of the lower peak. The upper peak could not be located because of the limited range of probe movement. Beyond the upper peak the pressure fluctuations would be expected to reduce to the free stream values. More detailed pressure measurements are required to determine the fin spatial pressure loading, and to relate this to the vortex burst pressure field.

6.4 Fin Response to Buffet Excitation

Using a single accelerometer mounted as shown in Figure 3, measurements were made of the port fin acceleration response to identify the conditions for maximum excitation. Surface pressure measurements were also made at a pressure port located close to the accelerometer. The pressure was transmitted through a 0.06 mm plastic tube to a transducer located on the fuselage inboard of the fin.

Prior to the wind-tunnel programme, vibration tests were carried out on the model fin to establish the frequency and the shape of the fin primary bending mode. Higher order modes were not investigated. The results of these tests are presented in Figure 15. It should be noted that during exploratory measurements cracks occurred in the fin mounting which resulted in the fin natural bending frequency reducing to a value of 68 Hz at the time of the test programme. The fin was not designed to match full scale stiffness and structural dynamic characteristics. However, since the frequency of the primary bending mode lies within the range of frequencies that occur in the vortex burst of the 1/9th scale model at normal tunnel speeds, excitation of the fin would be expected.

In general, the magnitude of the fin response will depend upon both the temporal and spatial distribution of energy in the pressure field with respect to the fin structural modes, and on the free stream dynamic pressures. The temporal distribution of energy in the pressure field was discussed in Section 6.2 where it was shown that the centre frequency of the energy associated with the vortex burst is a linear function of tunnel free stream velocity. It was also found (Section 6.2), that the centre frequency varies with angle of attack as well as with vortex burst position. The measurement of the spatial distribution of unsteady pressures on the fin has not been completed and so its influence cannot be assessed at this stage.

To account for the effects of free stream dynamic pressure the measurements of pressure and acceleration have been normalised with respect to dynamic pressure. The justification for this approach can be supported by reference to Figure 16, where the surface pressure measurements are presented in the form of a pressure coefficient. This coefficient is defined by Reference [1] using equation 1.

$$\bar{\bar{C}}_p = \left(\frac{4}{l\rho^2 V^3}\right)\bar{\bar{p}} \tag{1}$$

where

$\bar{\bar{C}}_p$	is the non-dimensional pressure coefficient PSD
$\bar{\bar{p}}$	is the measured pressure PSD
l	is a characteristic length (MAC)
ρ	is air density
V	is velocity

For the three angles of attack tested the coefficients are seen to vary only slightly with tunnel velocity. Further measurements are needed to establish the repeatability of these pressure peaks, particularly at low speeds. However, the accuracy is considered satisfactory for the current investigation.

In Figures 17 and 18, the value of the normalised pressure at the fin tip, measured from PSD curves at the fin natural frequency, and the peak normalised acceleration response show a similar variation with speed. From these figures, the peak fin response occurs between 35 and 40 m/sec for the 26.5° angle of attack case and at around 40 m/sec for the 31.5° angle of attack case. Note that the data in these figures are measured at 5 m/sec intervals and so the location of the peak values cannot be established accurately. Based on the frequency scaling results given in Section 6.2 and Figure 11, the tunnel free stream velocities at which the peak pressure frequency matches the fin natural frequency of 68 Hz are 35 m/sec for 26.5° angle of attack, and 40 m/sec for 31.5° angle of attack. These results indicate that when the effect of dynamic pressure is taken into account, the maximum normalized fin response occurs when the frequency of the peak pressure field and the fin natural frequency are approximately matched. Peak accelerations of the order of 120 g were recorded at the tip of the fin in the conditions of maximum excitation. This is compatible with a fin tip amplitude of 6.44 mm at the fin bending frequency of 68 Hz. The spatial distribution of pressures will also influence the fin response. However, further measurements of differential pressure loading would be required to determine the magnitude of this influence.

6.5 Fin Response as a Function of Sideslip

The acceleration response of the port fin tip was measured for a range of sideslip angles for 26.5° angle of attack and 50 m/sec tunnel velocity. Peak values of the power spectral density analysis are plotted in Figure 19 for the cases with LEX fence on and LEX fence off. With the LEX fence off the maximum response occurs at approximately −1.0° sideslip (ie. with the fin displaced outboard with respect to the LEX vortex) and significant fin response occurs over a sideslip range between −6° and +4°.

With the LEX fence fitted the fin response, shown as a peak power spectral density value, reduces substantially for this angle of attack and tunnel speed. The maximum value now occurs at around +3° sideslip angle.

6.6 Fin Differential Pressure Measurements

To obtain information on the spatial distribution of the fin pressure field, and its influence on fin structural response, simultaneous measurements are required at a matrix of points on each side of the fin. In the present series of tests only a small number of transducers were available and so exploratory measurements were made using two transducers mounted on the 10% chord line at three spanwise locations of 30%, 60% and 90%. The transducers were mounted obliquely through the fin such that their sensitive surfaces were directly opposite each other. A summing amplifier was used to calculate the differential pressure, and all three signals were analysed using the frequency analyser.

Peak values of the power spectral density results taken from thirty averages are shown in Figures 20 to 22 for each transducer and for the differential pressure. The data are presented as non-dimensional pressure coefficient PSD values as defined in equation 1.

The results show that the pressures on each surface and their variation with spanwise location and with angle of attack differ substantially. In general the inboard pressures are least at the 60% span location and increase towards the root and the tip. In contrast the outboard pressures are greatest at the 60% spanwise location, slightly less at the 30% location and are much smaller at the fin tip. The pressures at 30% and 60% span on the outboard surface increase significantly with increasing angle of attack. The differential pressure calculated as a root mean square (RMS) value can vary between zero, when the pressure fields on the inner and outer surfaces are unaltered by the presence of the fin, to a value equal to the sum of the separate pressures when the phase difference equals 180°. It can be seen that the presence of the fin modifies the pressure field considerably since in no case is the differential pressure zero and for the locations at 30% and 60% span, the sum of the separate RMS values on each side of the fin approaches the differential pressure value. Figure 23 summarises the spanwise variation in the differential pressures at the 10% chordwise position. With the exception of the results at 31.5° angle of attack, the magnitude of the net pressures decrease from root to tip and increase with increasing angle of attack.

These exploratory measurements indicate that the vortex burst pressure field is modified substantially as it passes over the fin. Both the distribution of pressures and the variation with angle of attack on the inboard and outboard surface differ significantly, and result in large differential pressures. The contribution to the differential pressure field due to vibration of the fin has not been determined.

6.7 Measurements with Wing Leading Edge Extension Fence Fitted

Some of the results for cases with the wing leading edge extension fence fitted were presented in previous sections. In this section the major changes due to the installation of the fence are summarised.

The tests indicated a marked change in the vortex burst unsteady pressure field. The magnitudes of the unsteady pressures, as shown in Figure 24, were reduced significantly while the frequency content extended over a wider band. The fin tip acceleration is significantly reduced with the fences fitted as shown in Figure 19 for the cases tested at an angle of attack case of 26.5° and varying sideslip angle.

Flow visualisation measurements showed little change in the longitudinal location of the vortex burst although the vertical location and general shape of the burst region was altered slightly. The pressure probe measurements taken at the same location as

those without the fence fitted, indicated a marked reduction in the magnitude and spatial variation of the pressure field in this region as shown in Figure 14. A search for regions of higher pressure intensity should be carried out in future tests.

With the fence in place, the flow visualisation measurements confirmed the existence of a second vortical structure emanating from the leading edge extension alongside the fence, as shown in Figure 25. The second structure interacts with the primary vortex and also exhibits bursting. A complete explanation for the flow interactions due to the presence of the fence and for the significant reduction in pressure field intensity due to this interaction has not yet been developed. Some flow visualisation results showing the effect of the fence have been obtained in a water tunnel and are described in Reference [4].

7 Conclusions

Exploratory measurements carried out using a small number of high frequency pressure transducers and a small accelerometer on a 1/9th scale wind-tunnel model have provided valuable insight into the character of the vortex burst and subsequent fin vibration on the F/A-18. Flow visualisation measurements with fin on and fin off show that the presence of the fin moves the vortex burst point upstream. Pressure measurements made on the wing surface below the vortex burst and on the fin show that the burst pressure field contains energy over a moderately narrow frequency band. The centre of the frequency band is a linear function of free stream velocity. Fin tip acceleration measurements show that the fin bending mode response is strongly coupled with the burst characteristic frequency and hence free stream velocity. The burst characteristic frequency is also modified when angle of attack is changed or when the fin is removed. Measurements made over a range of sideslip angles show that significant fin response occurs over a sideslip range between $\pm 6°$ with maximum excitation around $0°$. Exploratory measurements of the differential pressures acting on each side of the fin show that the vortex burst pressure field is modified as it passes over the fin. Although the frequency content is changed only slightly, the difference in magnitude and phase of the pressures on each side of the fin leads to substantial net pressure loads. Measurements made through the vortex burst using a small pressure probe indicated a uniform variation in unsteady pressure intensity. The profile was minimum at the point identified from flow visualisation measurements as the centre of the vortex burst and increased to maximum values at a radius of the order of the fin semi-span from this point before reducing to free stream values. Tests carried out with the leading edge extension fences fitted indicated a marked change in the vortex burst unsteady pressure field. The magnitude of the unsteady pressures was reduced significantly while the frequency content extended over a wider band. Fin tip acceleration, with the fences fitted, was significantly reduced. Flow visualisation measurements and burst profile probe pressure measurements indicated little change in the location of the vortex burst pressure field with the fences fitted, but a marked reduction in the magnitude and variation of the unsteady pressure field. The flow visualisation tests confirmed the existence of a second vortical structure emanating from the leading edge extension opposite the fence with the fence in place. The second structure interacts with the primary vortex and also exhibits bursting. An explanation for the significant reduction in pressure field intensity due to this interaction has not been developed. Further measurements are planned including comparisons with results from tests at different velocities and on different models to help characterisation of the vortex burst structure.

Acknowledgements

The advice and suggestions of Dr B. D. Fairlie, Mr N. Pollock, Dr D. H. Thompson, and Dr J. Lopez of the Flight Mechanics Branch and P. A. Farrell of the Structures Division ARL during the test programme is acknowledged. Significant instrumentation support was provided by Aircraft Structures Division and Aircraft Propulsion Branch and is gratefully acknowledged, as are the efforts of the Flight Mechanics technical staff.

References

[1] Zimmerman, N. H. and Ferman, M. A., 'Prediction of Tail Buffet Loads for Design Applications. Vols I and II', Naval Air Development Center Report, NADC 88043-60, July 1987.

[2] Lee, B. H. K. and Brown D., 'Wind Tunnel Studies of F/A-18 Tail Buffet', AIAA Paper No. 90-1432, AIAA 16th Aerodynamic Ground Testing Conference, Seattle WA, June 1990.

[3] MacLaren, L. D. and Hill, S. D., 'A Fortran Program for Spectral Analysis using the Fast Fourier Transform', Flight Mechanics Technical Memorandum 432, Aeronautical Research Laboratory, Melbourne Australia, March 1991.

[4] Thompson, D. H., 'Water Tunnel Flow Visualisation of Vortex Breakdown Over the F/A-18', Flight Mechanics Report 179, Aeronautical Research Laboratory, Melbourne Australia, October 1990.

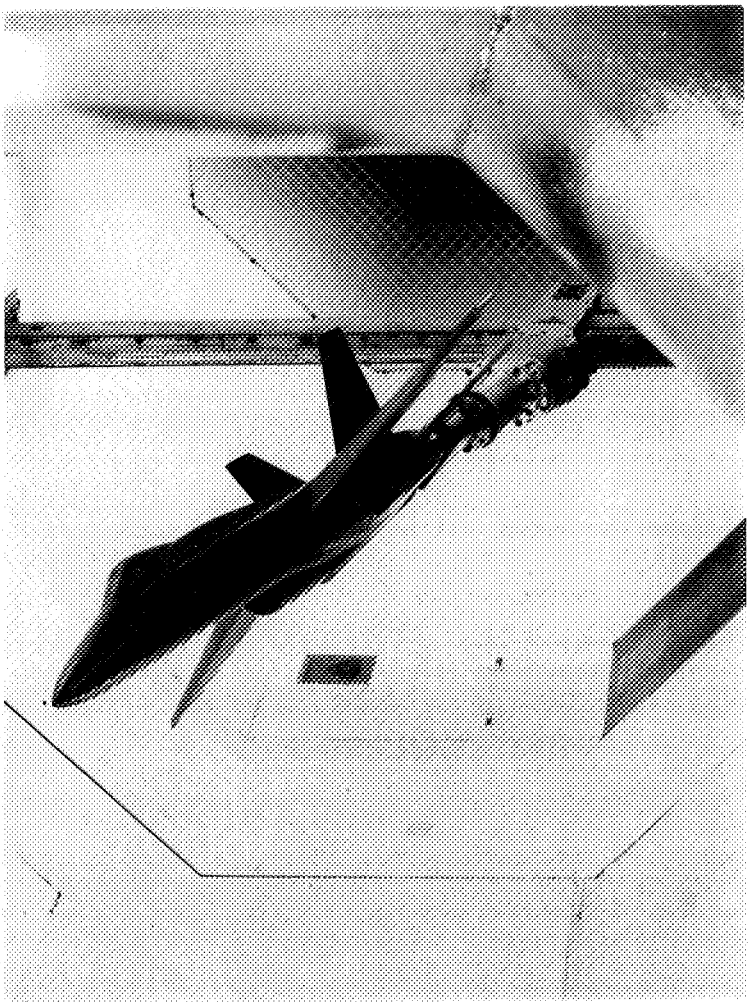

FIGURE 1. Photograph of 1/9th scale F/A-18 model

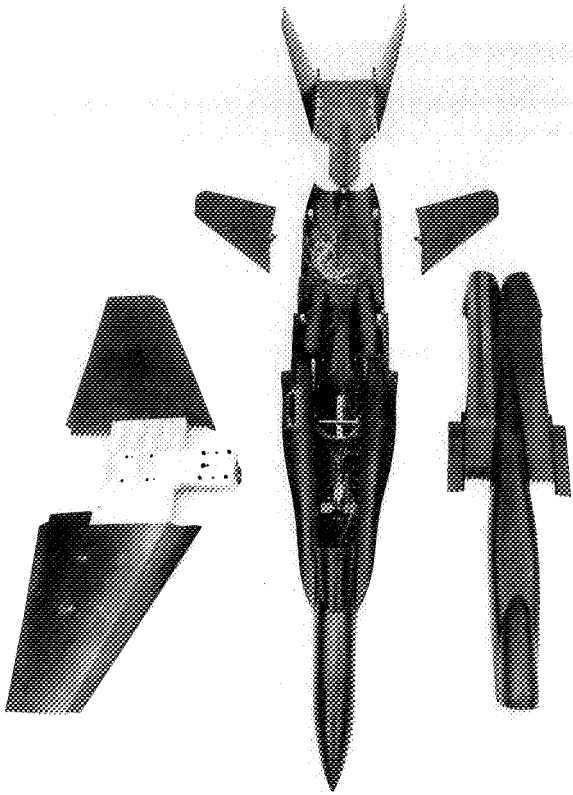

Figure 2. Sub-assemblies of 1/9th scale F/A-18 model

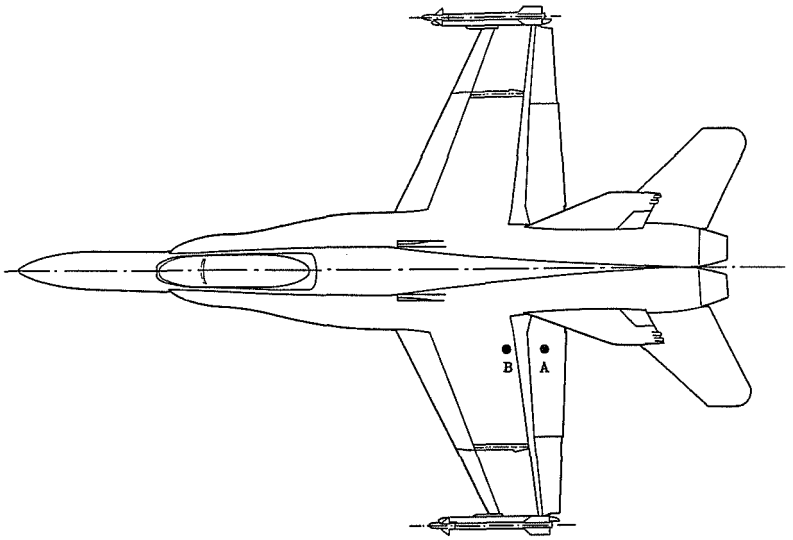

□ Port fin accelerometer;
60% chord, 93% span

○ Port fin differential pressure tappings;
10% chord, 30, 60, and 90% span

● Port fin outboard pressure tapping;
64% chord, 90% span

⊗ Wing surface mounted pressure transducers;
31% span port of A/C centreline,
71.8% (A) and 66.6% (B) of A/C length

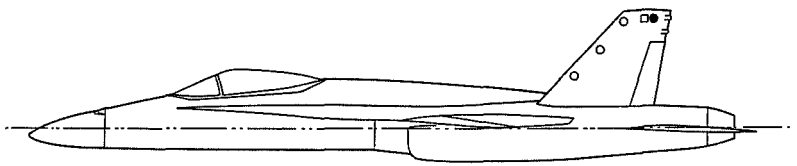

Figure 3. Location of pressure tappings and transducers

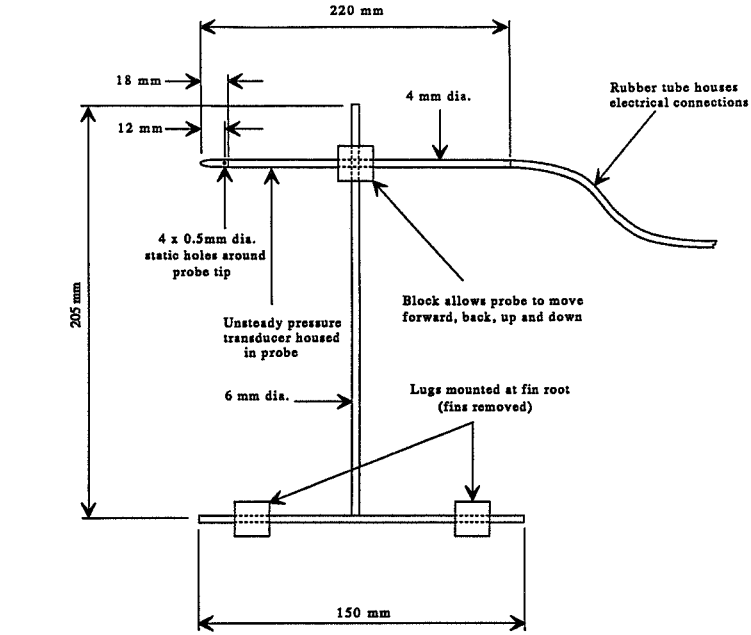

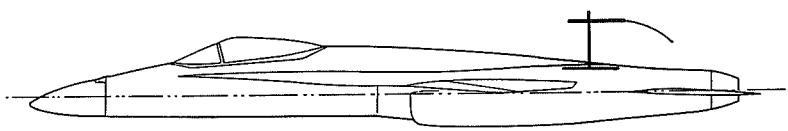

Figure 4. Diagram of static probe assembly

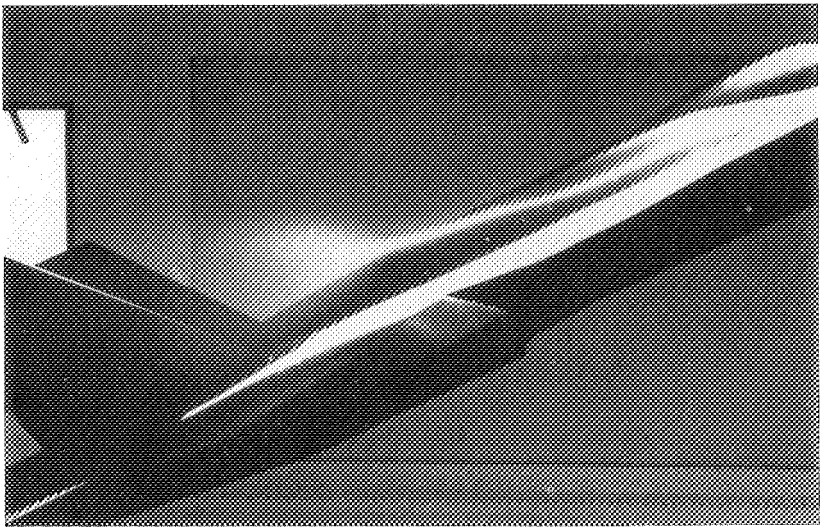

Fins on, 23.5 degrees angle of attack

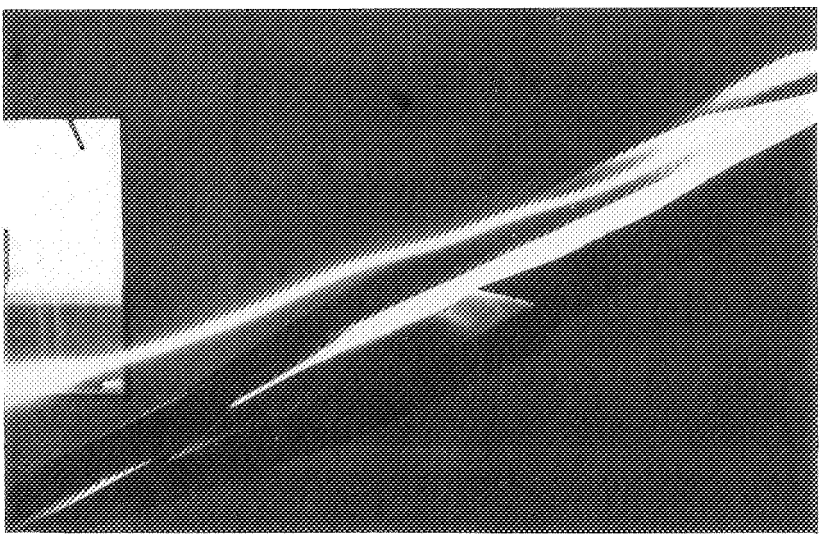

Fins off, 23.5 degrees angle of attack

FIGURE 5. Example of vortex burst flow visualisation using smoke

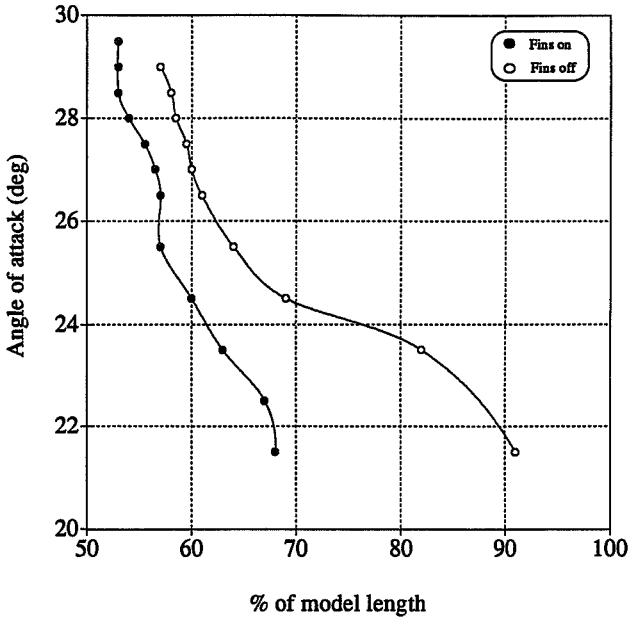

Figure 6. Location of vortex burst position

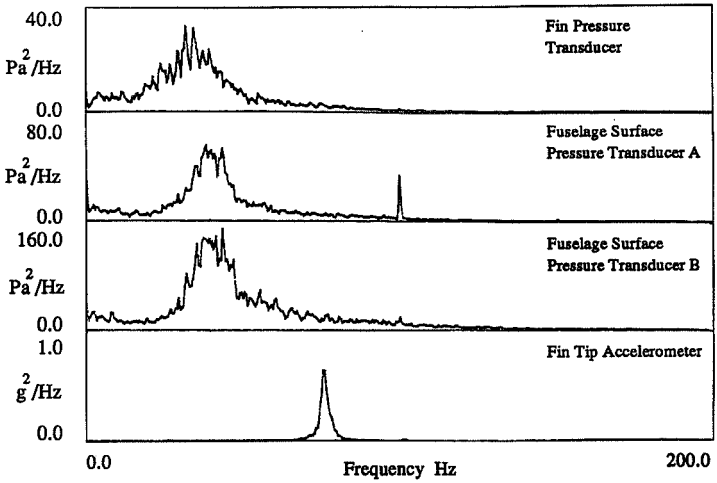

Figure 7. Power Spectral Density results for 26.5 deg angle of attack and tunnel speed 20 m/s

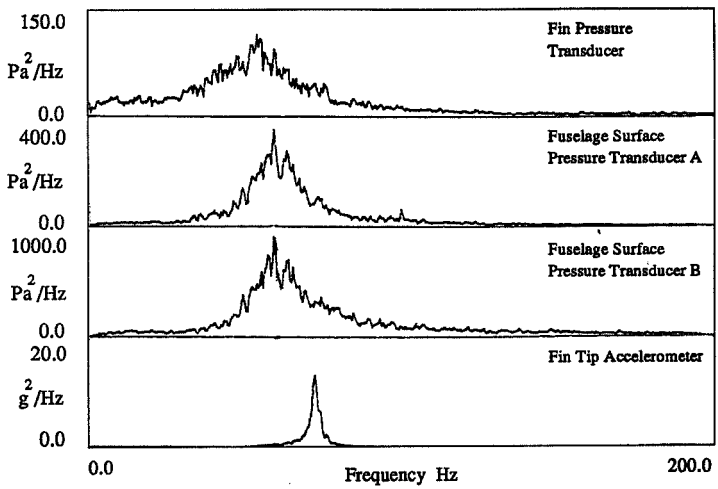

Figure 8. Power Spectral Density results for 26.5 deg angle of attack and tunnel speed 30 m/s

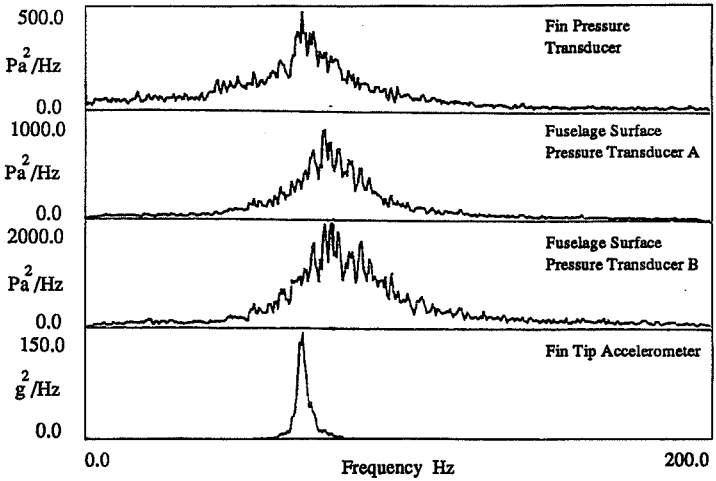

Figure 9. Power Spectral Density results for 26.5 deg angle of attack and tunnel speed 40 m/s

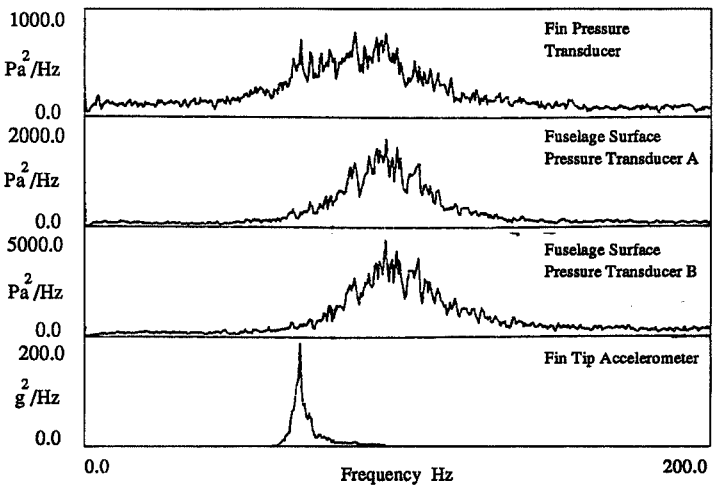

Figure 10. Power Spectral Density results for 26.5 deg angle of attack and tunnel speed 50 m/s

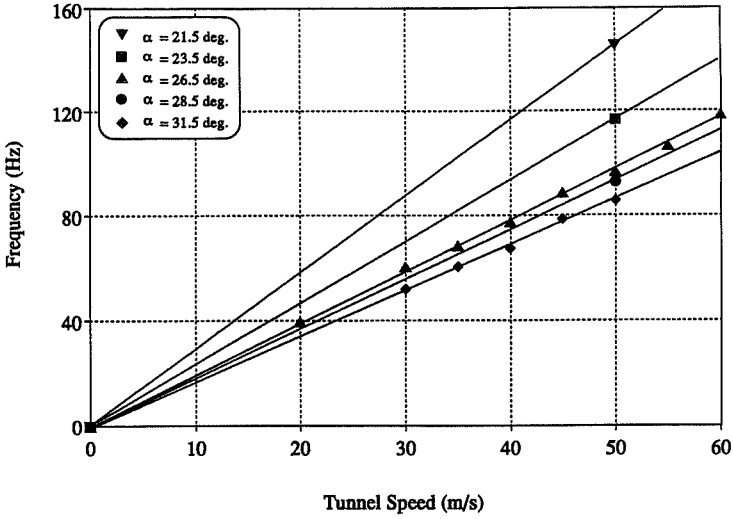

Figure 11. Variation of vortex burst frequency with tunnel speed - fins on

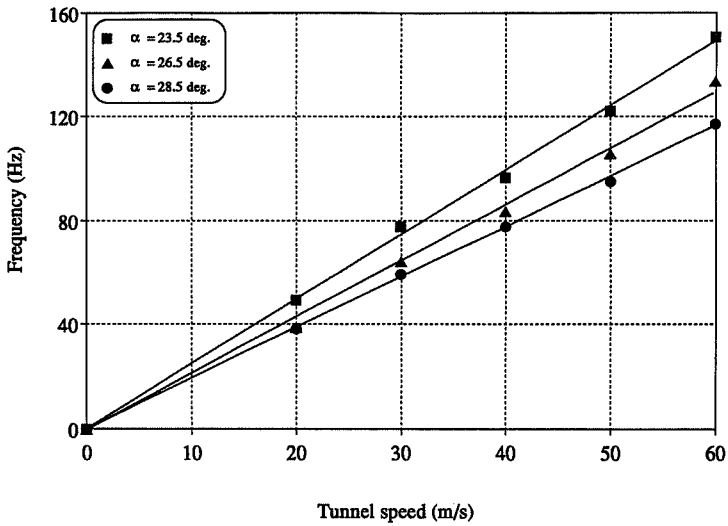

Figure 12. Variation of vortex burst frequency with tunnel speed - fins off

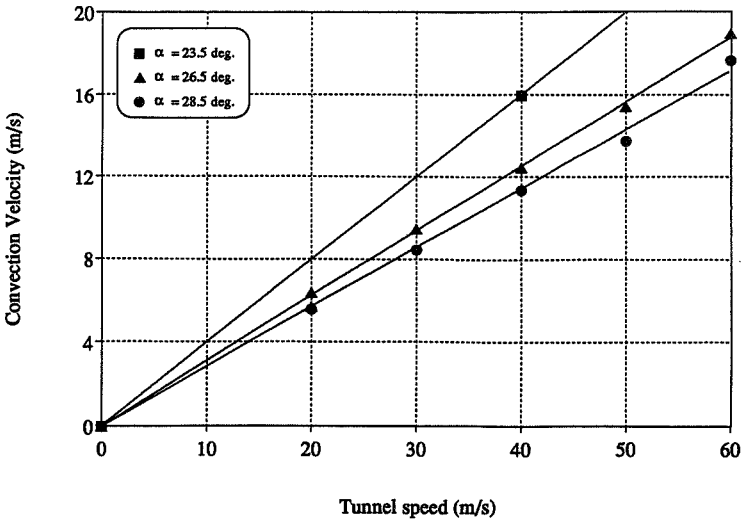

Figure 13. Variation of pressure field convection velocity with tunnel speed - fins off

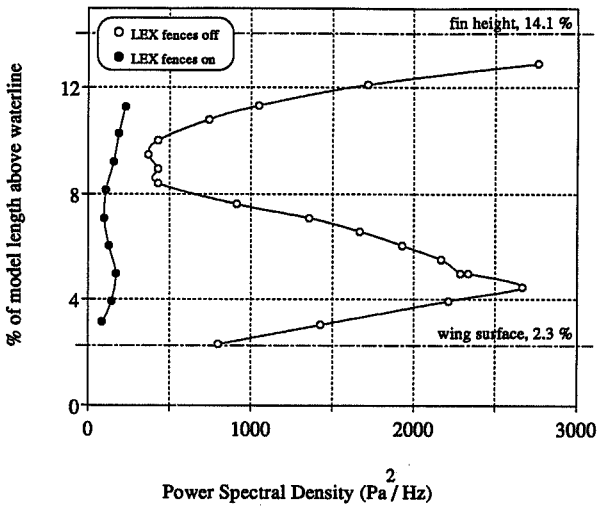

Figure 14. Power Spectral Density of pressure probe measurements through vortex burst; Traverse parallel to model normal axis. α = 26.5 deg, V = 50 m/s

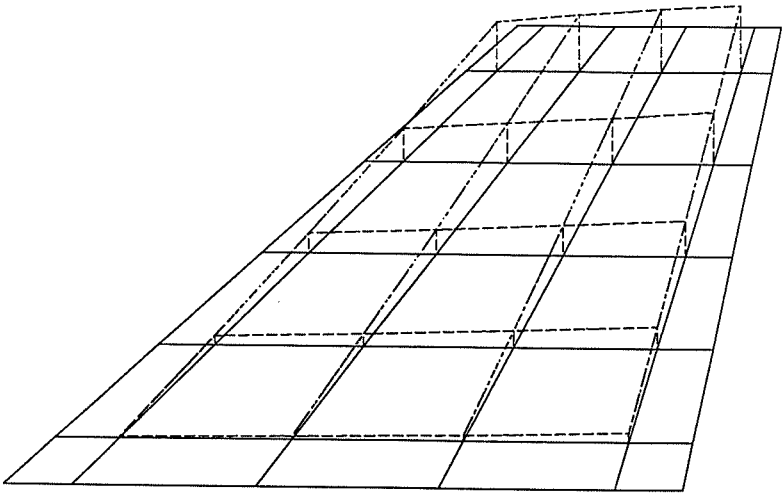

Figure 15. 1/9th scale F/A-18 wind tunnel model fin mode shape from vibration tests

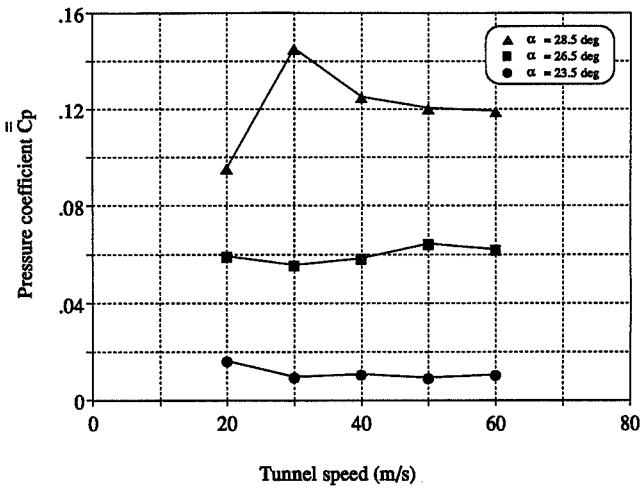

Figure 16. Power Spectral Density surface pressure measurements in coefficient form

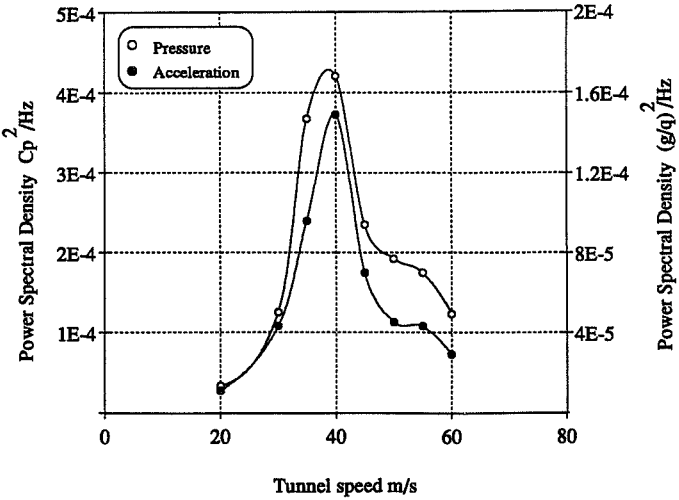

Figure 17. Port-fin tip surface pressure and acceleration measurements; angle of attack 26.5 degrees - variation with tunnel speed

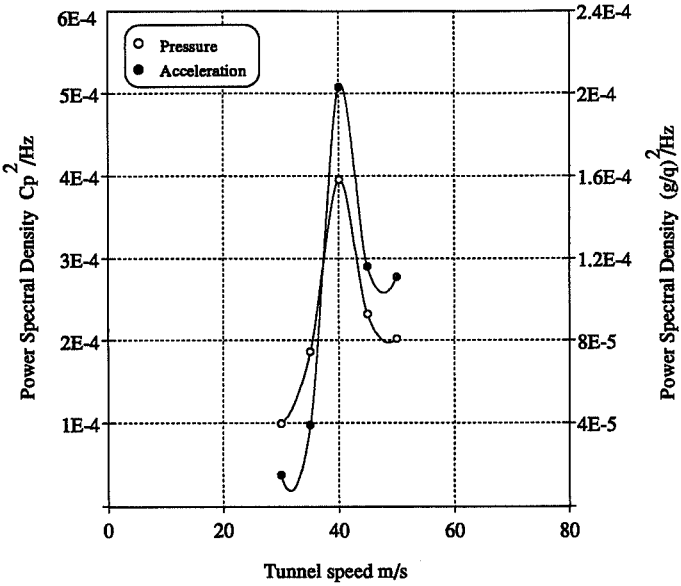

Figure 18. Port-fin tip surface pressure and acceleration measurements; angle of attack 31.5 degrees - variation with tunnel speed

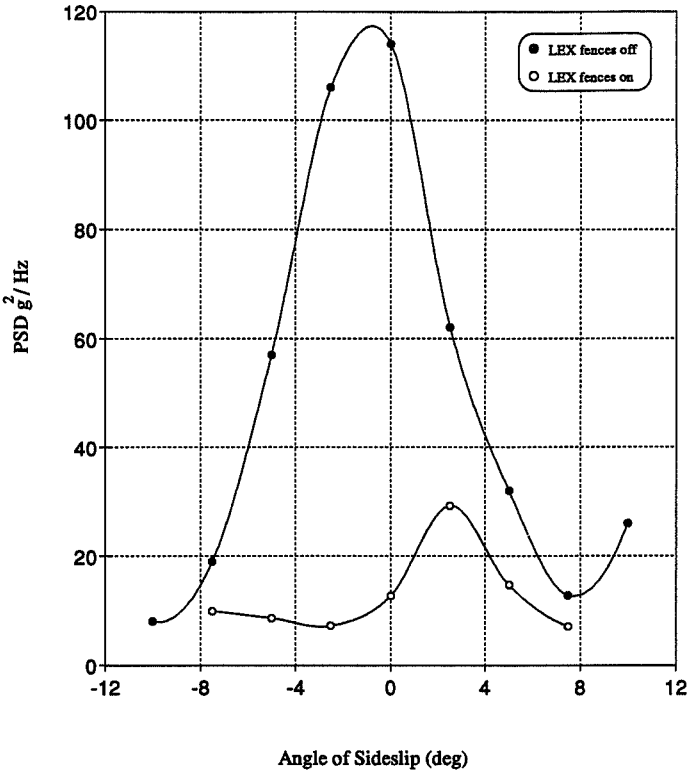

Figure 19. Power Spectral Density of port fin-tip acceleration measurements at 26.5 degrees angle of attack and 50 m/sec tunnel speed; variation with sideslip angle

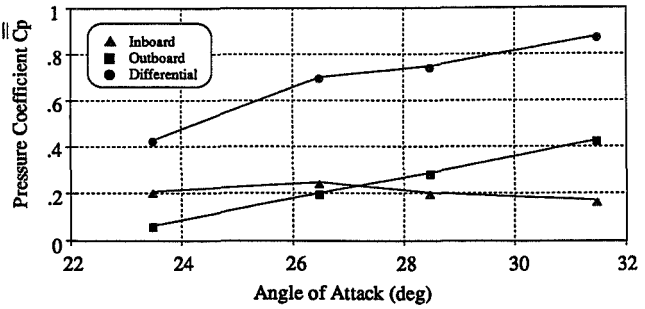

Figure 20. Pressure coefficient variation on port fin;
10 % chord, 30 % span, tunnel speed 50 m/sec

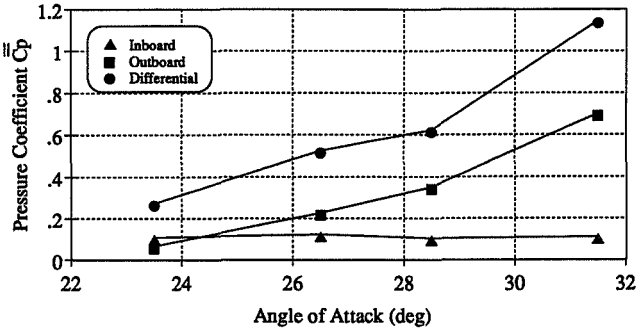

Figure 21. Pressure coefficient variation on port fin;
10 % chord, 60 % span, tunnel speed 50 m/sec

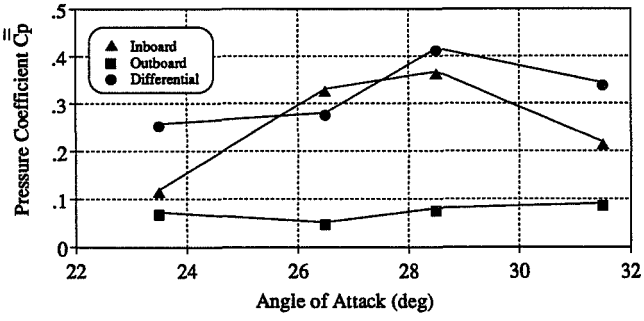

Figure 22. Pressure coefficient variation on port fin;
10 % chord, 90 % span, tunnel speed 50 m/sec

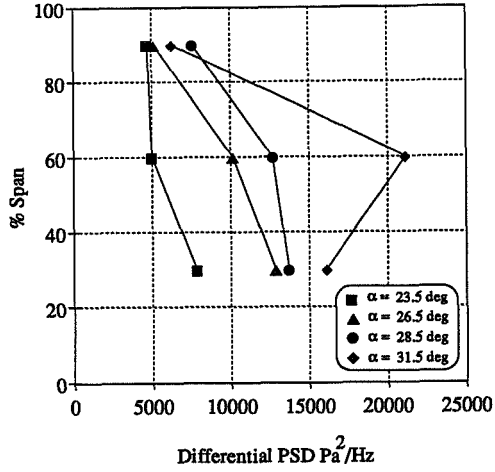

Figure 23. Differential fin pressures at 10 % chord, tunnel speed 50 m/s

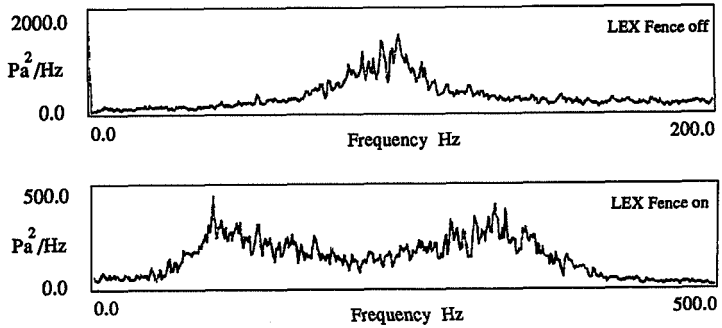

Figure 24. Fin pressures at 50% span and 90% chord for LEX fence on/off. Angle of attack 26.5 deg. and tunnel speed 50 m/s

Figure 25. Visualisation of vortex flow with LEX fences fitted

DISTRIBUTION

AUSTRALIA

Department of Defence

Defence Central
- Chief Defence Scientist)
- AS, Science Corporate Management) shared copy
- FAS Science Policy)
- Director, Departmental Publications
- Counsellor, Defence Science, London (Doc Data Sheet Only)
- Counsellor, Defence Science, Washington (Doc Data Sheet Only)
- S.A. to Thailand MRD (Doc Data Sheet Only)
- S.A. to the DRC (Kuala Lumpur) (Doc Data Sheet Only)
- OIC TRS, Defence Central Library
- Document Exchange Centre, DSTIC (8 copies)
- Defence Intelligence Organisation
- Librarian H Block, Victoria Barracks, Melbourne

Aeronautical Research Laboratory
- Director
- Library
- Chief Flight Mechanics and Propulsion
- Head, Flight Mechanics Branch
- Branch File, Flight Mechanics Branch
- Authors: C.A. Martin (1 copy + 7 copies for TTCP HTP-5)
  - M.K. Glaister
  - L.D. MacLaren
- D.H. Thompson
- B.D. Fairlie
- N. Pollock

Materials Research Laboratory
- Director/Library

Defence Science & Technology Organisation - Salisbury
- Library

Navy Office
- Navy Scientific Adviser (3 copies Doc Data sheet)

Army Office
- Scientific Adviser - Army (Doc Data sheet only)
- Engineering Development Establishment Library

Air Force Office
Air Force Scientific Adviser (Doc Data sheet only)
Aircraft Research and Development Unit
Scientific Flight Group
Library
Director General Engineering - Air Force
AHQ (SMAINTSO)
HQ Logistics Command (DGLOGENG)

HQ ADF
Director General Force Development (Air)

Statutory and State Authorities and Industry
Aero-Space Technologies Australia, Systems Division Librarian
Hawker de Havilland Aust Pty Ltd, Bankstown, Library

CANADA
IAR Ottawa
Dr B.M.K. Lee

UNITED STATES OF AMERICA
NASA Scientific and Technical Information Facility
NASA Ames Research Center
Library
L.A. Meyn
J. Ross
NASA Langley Research Center, Library
McDonnell Aircraft Company
Library
Mr R.J. Paul (F/A-18 Aerodynamics)
Naval Air Systems Command Headquarters
Mr R.J. Hanley (F/A-18 Aerodynamics)

SPARES (10 COPIES)

TOTAL (61 COPIES)

AL 149 DEPARTMENT OF DEFENCE

DOCUMENT CONTROL DATA

PAGE CLASSIFICATION
UNCLASSIFIED

PRIVACY MARKING

1a. AR NUMBER	1b. ESTABLISHMENT NUMBER	2. DOCUMENT DATE	3. TASK NUMBER
AR-006-149	ARL-FLIGHT-MECH-R-188	JUNE 1991	DST 90/061

4. TITLE
F/A-18 1/9TH SCALE MODEL

TAIL BUFFET MEASUREMENTS

5. SECURITY CLASSIFICATION (PLACE APPROPRIATE CLASSIFICATION IN BOX(S) IE. SECRET (S), CONF. (C) RESTRICTED (R), UNCLASSIFIED (U)).

DOCUMENT	TITLE	ABSTRACT
U	U	U

6. NO. PAGES
29

7. NO. REFS.
3

8. AUTHOR(S)
C.A. MARTIN, M.K. GLAISTER,
L.D. MACLAREN (ARL)
L.A. MEYN, J. ROSS (NASA AMES)

9. DOWNGRADING/DELIMITING INSTRUCTIONS
Not applicable

10. CORPORATE AUTHOR AND ADDRESS
AERONAUTICAL RESEARCH LABORATORY
506 LORIMER STREET
FISHERMENS BEND VIC 3207

11. OFFICE/POSITION RESPONSIBLE FOR:
SPONSOR DST
SECURITY -
DOWNGRADING -
APPROVAL DARL

12. SECONDARY DISTRIBUTION (OF THIS DOCUMENT)

Approved for public release

OVERSEAS ENQUIRIES OUTSIDE STATED LIMITATIONS SHOULD BE REFERRED THROUGH DSTIC, ADMINISTRATIVE SERVICES BRANCH, DEPARTMENT OF DEFENCE, ANZAC PARK WEST OFFICES, ACT 2601

13a. THIS DOCUMENT MAY BE ANNOUNCED IN CATALOGUES AND AWARENESS SERVICES AVAILABLE TO ....

No limitations

13b. CITATION FOR OTHER PURPOSES (IE. CASUAL ANNOUNCEMENT) MAY BE [X] UNRESTRICTED OR [ ] AS FOR 13a.

14. DESCRIPTORS

F/A-18 aircraft	Buffeting
Wind tunnel tests	Vortices
High angle of attack	Flow visualization
Leading edges	

15. DISCAT SUBJECT CATEGORIES
010301
010101

16. ABSTRACT

Wind-tunnel tests have been carried out on a 1/9th scale model of the F/A-18 at high angles of attack to investigate the characteristics of tail buffet due to bursting of the wing leading edge extension (LEX) vortices. The tests were carried out at the Aeronautical Research Laboratory low-speed wind-tunnel facility and form part of a collaborative activity with NASA Ames Research Center, organised by The Technical Cooperative Programme (TTCP). Information from the programme will be used in the planning of similar collaborative tests, to be carried out at NASA Ames, on a full-scale aircraft. The programme covered the measurement of unsteady pressures and fin vibration for cases with and without the wing LEX fences, designed by McDonnell Aircraft Company, fitted. Fourier transform methods have been used to analyse the unsteady data, and information on the spatial and temporal content of the vortex burst pressure field has been obtained. Flow visualisation of the vortex behaviour was carried out using smoke and a laser light sheet technique.

PAGE CLASSIFICATION
UNCLASSIFIED
PRIVACY MARKING

THIS PAGE IS TO BE USED TO RECORD INFORMATION WHICH IS REQUIRED BY THE ESTABLISHMENT FOR ITS OWN USE BUT WHICH WILL NOT BE ADDED TO THE DISTIS DATA UNLESS SPECIFICALLY REQUESTED.

16. ABSTRACT (CONT).

17. IMPRINT

AERONAUTICAL RESEARCH LABORATORY, MELBOURNE

18. DOCUMENT SERIES AND NUMBER	19. COST CODE	20. TYPE OF REPORT AND PERIOD COVERED
Flight Mechanics Report 188	525 120	

21. COMPUTER PROGRAMS USED

22. ESTABLISHMENT FILE REF.(S)

23. ADDITIONAL INFORMATION (AS REQUIRED)